PHYSICAL REVIEW B VOLUME 53, NUMBER 2 1 JANUARY 1996-II

Interference between Judd-Ofelt and Wybourne-Downer mechanisms in the $^5D_0$-^7F_J $(J=2,4)$ transitions of Sm^{2+} in solids

Masanori Tanaka and Takashi Kushida
Department of Physics, Osaka University, Toyonaka, Osaka 560, Japan

(Received 11 September 1995)

The strengths of the $^5D_0$-^7F_J $(J=0,2,4)$ optical transitions of the Sm^{2+} ion in solids, which are due to the forced electric dipole transition, are analyzed by taking into account not only the Judd-Ofelt mechanism but also the excited-state spin-orbit interaction (Wybourne-Downer) mechanism. The fact that the $^5D_0$-$^7F_0$ transition strength of the Sm^{2+} ion is much larger than that of the isoelectronic Eu^{3+} ion in various crystalline and glassy matrices is ascribed to the resonance effect which results from the presence of the $4f^55d$ states of Sm^{2+} in the vicinity of the $4f^6$ states concerned with the optical transition. However, such an enhancement of the transition strength due to the energetic resonance between the $4f^6$ and $4f^55d$ states is not observed in the $^5D_0$-$^7F_{2,4}$ transitions of Sm^{2+} in solids. This is identified as due to the interference between the Judd-Ofelt and Wybourne-Downer mechanisms.

I. INTRODUCTION

Both of the Eu^{3+} and Sm^{2+} ions have the $4f^6$ electron configuration, and the lower electronic energy-level structure is almost the same for these ions. However, the states of the $4f^55d$ configuration of Sm^{2+} are much closer in energy to the $4f^6$ states compared with the case of the Eu^{3+} ion,[1–6] and the energy of the lowest $4f^55d$ state of Sm^{2+} in solids is so low as to overlap with the ^5D_J states of the $4f^6$ electron configuration. We are interested in the effect of such a difference of the energy positions of the high-lying configuration states of Eu^{3+} and Sm^{2+} on their f-f optical transitions.[7] In this paper, we analyze the strengths of the $^5D_0(4f^6)$-$^7F_J(4f^6)$ $(J=0,2,4)$ transitions of Sm^{2+} in solids on the basis of both the Judd-Ofelt[8,9] and Wybourne-Downer theories[10–12] which were proposed to account for the electric dipole f-f transition of the rare-earth ion. The dynamic coupling model[13] has also been proposed as an additional mechanism for the f-f transitions which satisfy the selection rule $|J-J'|\leqslant t\leqslant J+J'$ $(t=2,4,6)$, where J and J' denote the inner quantum numbers for the initial and final states of the transition. However, since the transition matrix element in the dynamic coupling model is independent of the high-lying states of rare-earth ions, we do not consider the contribution of this model.

In this analysis, we use the experimental data on the same transitions of the isoelectronic Eu^{3+} ion in solids as references. The above transition strengths in Sm^{2+} are shown to be understood well by taking into account the small energy separations between the $4f^6$ and the $4f^55d$ states.

Most researchers have so far analyzed the optical spectra due to the f-f transitions of the rare-earth ion in condensed matter by means of only the Judd-Ofelt theory, and the Wybourne-Downer mechanism, which occurs through the spin-orbit interaction within the high-lying configuration states, does not appear to spread widely. However, it is shown in this paper that the Wybourne-Downer mechanism makes important contributions to the $^5D_0$-^7F_J $(J=0,2,4)$ transition strengths of Sm^{2+} in solids.

II. THEORY

Let us consider the electric dipole transition between the two $4f^N$ states of a rare-earth ion in condensed matter. We express the wave functions of these states under Russell-Saunders approximation as $|a\rangle$ and $|b\rangle$. When the total spin S is different by one unit between these states, as in the case of the $^5D_0$-^7F_J transitions of Sm^{2+} and Eu^{3+}, the transition matrix element is given by the sum of the two terms due to the Judd-Ofelt (JO) and Wybourne-Downer (WD) mechanisms as follows:

$$T(a\rightarrow b)=T_{\mathrm{JO}}(a\rightarrow b)+T_{\mathrm{WD}}(a\rightarrow b) \tag{1}$$

with

$$T_{\mathrm{JO}}(a\rightarrow b)=-\sum_m \left\{\frac{\langle[b]|\mathbf{P}|m\rangle\langle m|V_c^{\mathrm{odd}}|[a]\rangle}{E(m)-E([a])}+\frac{\langle[b]|V_c^{\mathrm{odd}}|m\rangle\langle m|\mathbf{P}|[a]\rangle}{E(m)-E([b])}\right\} \tag{2}$$

and

$$T_{\mathrm{WD}}(a\rightarrow b)=\sum_{m,m'}\left[\frac{\langle b|\mathbf{P}|m'\rangle\langle m'|H_{\mathrm{so}}|m\rangle\langle m|V_c^{\mathrm{odd}}|a\rangle}{\{E(m')-E(a)\}\{E(m)-E(a)\}}+\frac{\langle b|V_c^{\mathrm{odd}}|m'\rangle\langle m'|H_{\mathrm{so}}|m\rangle\langle m|\mathbf{P}|a\rangle}{\{E(m')-E(b)\}\{E(m)-E(b)\}}\right], \tag{3}$$

where $\mathbf{P}$ is the electric dipole moment, m and m' represent the high-lying states of the ion with the parity opposite to the $4f^N$ configuration, and $E(\gamma)$ is the energy of the γ state. Further, V_c^{odd} and H_{so} are the odd-parity components of the crystal-field potential acting on the rare-earth ion and the spin-orbit interaction, respectively. The intermediate-coupling approximation is used for the wave functions in [. . .], in order to take into account the spin-orbit interaction acting within the $4f^N$ states, which leads to the relaxation of the spin-selection rule $\Delta S=0$ in Eq. (2), and consequently makes the $\Delta S=1$ transition possible. In the case of Eq. (3),

0163-1829/96/53(2)/588(6)/$06.00

on the other hand, the $\Delta S=1$ transition is allowed even by using the pure Russell-Saunders states, because the spin-selection rule is relaxed by the spin-orbit interaction within the high-lying states which admix into the $4f^N$ states through the odd-parity crystal-field components. Furthermore, $T_{\mathrm{JO}}(a\rightarrow b)$ has only one energy denominator, while $T_{\mathrm{WD}}(a\rightarrow b)$ includes two. For this reason, the absolute value of the transition matrix element due to the Wybourne-Downer mechanism is much more sensitive to the energy positions of the opposite parity states than that due to the Judd-Ofelt mechanism. Accordingly, the Wybourne-Downer mechanism is predicted to make relatively large contributions to the f-f transitions in Sm^{2+} compared with Eu^{3+}.

Both of Judd-Ofelt and Wybourne-Downer theories adopted the closure approximation to the high-lying states m and m' in Eqs. (2) and (3) in order to proceed with the calculations of the transition matrix elements. As a result, the $J=0\leftrightarrow J'=0$ transition, such as the ${}^5D_0$-${}^7F_0$ transition of Sm^{2+} and Eu^{3+}, is forbidden in the Judd-Ofelt theory, although it is allowed by the Wybourne-Downer mechanism. On the other hand, the $J=0\leftrightarrow J'=2,4,6$ transitions, such as the ${}^5D_0$-${}^7F_{2,4}$ transitions are permitted by both mechanisms.

If we employ the closure approximation, the ${}^5D_0$-${}^7F_3$ transition is strictly forbidden in the Judd-Ofelt mechanism and only a weak intensity is predicted for this transition by the Wybourne-Downer theory.[12] Actually, this transition in the Sm^{2+}-doped solids is usually observed only weakly,[2–4,14] whose presence may be explained by the J-mixing effect, i.e., the mixing of the $4f^N$ states of the same parity through the even-parity crystal-field components. Thus, the breakdown of the closure approximation does not appear to be so serious even in Sm^{2+}. Therefore, we adopt this approximation in the following analysis.

III. ANALYSIS AND DISCUSSION

The ${}^5D_0$-${}^7F_1$ transition of Sm^{2+} and Eu^{3+} is forbidden by both the Judd-Ofelt and Wybourne-Downer mechanisms, and it is due to the parity-allowed magnetic dipole transition.[1,15] Accordingly, its strength is considered to be almost independent of the energy separation between the $4f^6$ and higher-energy configurations and also of the crystal-field strength acting on the rare-earth ions. In addition, the squared transition matrix elements are almost equal in magnitude for this transition of the Sm^{2+} and Eu^{3+} ions, because the wave functions of the ${}^5D_0$ and ${}^7F_1$ states in the intermediate-coupling scheme are nearly the same between these ions.[16] Accordingly, the ${}^5D_0$-${}^7F_1$ fluorescence intensity of these ions can be used as a standard. Keeping this fact in mind, we have compared the fluorescence spectra of Eu^{3+} and Sm^{2+} in various host materials.[17,18] As a consequence, we have noticed the following points:

(i) The ${}^5D_0$-${}^7F_0$ transition strength of Sm^{2+} is much larger than that of Eu^{3+} in most host matrices.

(ii) On the other hand, the fluorescence intensity due to the ${}^5D_0$-${}^7F_2$ transition of the Sm^{2+}-doped materials is weaker than that of the Eu^{3+}-doped samples or comparable to it. As typical examples, we show the fluorescence spectra of Sm^{2+}-doped and Eu^{3+}-doped fluoride glasses in Figs. 1(a) and 1(b), respectively.

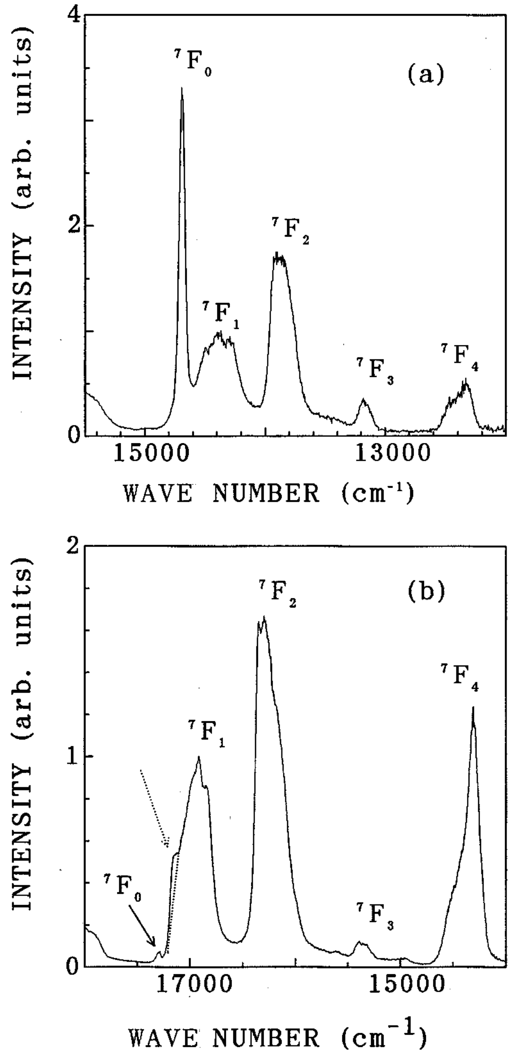

FIG. 1. Fluorescence spectra at 300 K due to the ${}^5D_0$-${}^7F_J$ transitions of (a) Sm^{2+} in HBLAN fluoride glass [(53)HfF_4, (20)BaF_2, (4)LaF_3,(3)AlF_3,(20)NaF] and (b) Eu^{3+} in ZBL fluoride glass [(60.6)ZrF_4,(33.3)BaF_2,(6.1)LaF_3]. Here, the numbers in the round brackets denote the mole ratios for the compositions. The excitations have been made by all lines of an Ar^+ laser for (a) and its 465.8 nm line for (b), respectively. The dotted arrow in (b) denotes the ${}^5D_1$-${}^7F_3$ transition. Corrections have been made for the wavelength dependence of the transmittance of the monochromator and the sensitivity of the photodetector.

When the closure approximation is used for the high-lying states, the transition matrix element (3) can be nonzero for the ${}^5D_0$-${}^7F_0$ transition through the $k=1$ term (linear term) of the crystal-field potential at the rare-earth ion site, which is written in the form

$$V_c=\sum_{k,q,i} B_{kq}C_{kq}(\theta_i,\phi_i) \tag{4}$$

with $C_{kq}(\theta_i,\phi_i)=\sqrt{4\pi/(2k+1)}Y_{kq}(\theta_i,\phi_i)$. Here, $Y_{kq}(\theta_i,\phi_i)$ is the q component of the kth-order spherical harmonics, and (r_i,θ_i,ϕ_i) represents the position of the ith $4f$ electron of the rare-earth ion. There exists another mechanism of this transition due to the J mixing. Actually, it has been proved by our group[19] that the dominant mechanism of the ${}^5D_0$-${}^7F_0$ transition of Eu^{3+} in oxide glasses is to borrow intensity by the J-mixing effect through the second-order crystal-field potential from the ${}^5D_0$-${}^7F_2$ transition, which is permitted by the Judd-Ofelt and Wybourne-Downer mechanisms. This J-mixing effect will also account for the ${}^5D_0$-${}^7F_0$ transition of the Eu^{3+} ion in fluoride glass. In the case of Sm^{2+} in fluoride glass, on the other hand, this transition is too intense to be explained by the J-mixing effect, and the Wybourne-Downer mechanism is considered to contribute dominantly to the ${}^5D_0$-${}^7F_0$ transition strength.

There exist two probable causes which account for the difference in the dominant mechanism of the ${}^5D_0$-${}^7F_0$ transition between Sm^{2+} and Eu^{3+} in fluoride glass. One is the difference in the magnitude of the linear term of the crystal-field potential at the rare-earth ion site, and the other is the difference in the energy positions of the high-lying odd-parity states relative to the ${}^5D_0$ and ${}^7F_0$ states. As is evident from expression (3), the lower energies of the high-lying odd-parity states lead to higher intensities of the ${}^5D_0$-${}^7F_0$ transition.

In the case of Eu^{3+} in condensed matter, the charge-transfer states make more effective contribution to the electric-dipole f-f transition than the $4f^5 5d$ states as intermediate states, m and m', in expressions (2) and (3),[5] because the energies of the charge-transfer states are usually lower than those of the $4f^5 5d$ states in the Eu^{3+}-doped materials.[6] However, the energies of the $4f^5 5d$ states of the Sm^{2+} ion are usually located much lower in energy compared with the charge-transfer states of the Eu^{3+} ion. For example, in the case of the Eu^{3+} ion in fluoride host matrices, the charge-transfer band, which is considered to be due to the transition in which one $2p$ electron of the surrounding F^- transfers to the $4f$ orbital of the Eu^{3+} ion, lies in the vacuum ultraviolet region, while the absorption band due to the parity-allowed f-d transitions of Sm^{2+} in fluoride glass appears from the visible to the ultraviolet region, as shown in Ref. 4. On the other hand, it is not probable that the linear term of the crystal-field potential is much different between Eu^{3+} and Sm^{2+} in similar fluoride glass hosts. Accordingly, the remarkable difference in the ${}^5D_0$-${}^7F_0$ transition strength between the Sm^{2+}- and Eu^{3+}-doped glasses in Figs. 1(a) and 1(b) is ascribed to the difference in the resonance effect between the high-lying states and the $4f^6$ states concerned with the transition. The similar analyses account well for the result (i) in other kinds of host matrices.

It has been reported that the Eu^{3+} ion in several oxide matrices exceptionally has such a strong ${}^5D_0$-${}^7F_0$ line as to be comparable to that line in the Sm^{2+}-doped samples.[20] The charge-transfer states of such Eu^{3+}-doped materials are known to be fairly low in energy compared with those in ordinary oxide hosts.[5] In addition, it has been pointed out that the linear term of the crystal-field potential is relatively large in these materials.[20]

The ${}^5D_0$-${}^7F_2$ transition is allowed to occur as the electric dipole transition by both the Judd-Ofelt and Wybourne-Downer mechanisms. Thus, the strength of this transition of Sm^{2+} in solids is also expected to be enhanced by the above resonance. However, the characteristic of (ii) mentioned above shows that such an enhancement is not observed in the ${}^5D_0$-${}^7F_2$ transition of the Sm^{2+}-doped materials. Next, we discuss the cause of this on the basis of expressions (1)–(3).

Here, we calculate the transition matrix element (1) for the ${}^5D_0$-${}^7F_2$ transition of the Sm^{2+} ion in solids. As mentioned above, the $\Delta S = 1$ transition due to the Wybourne-Downer mechanism is possible to occur even if we adopt the pure Russell-Saunders states as the $4f^6$ states. However, the ${}^5D_0$ state includes the ${}^7F_0$ component considerably by the spin-orbit interaction within the $4f^6$ configuration states, although the L-S coupling approximation holds fairly well for the ${}^7F_2$ state.[16] For this reason, we use the intermediate-coupled wave function calculated by Ofelt[16] only for the ${}^5D_0$ state, while regarding the ${}^7F_2$ state as a pure Russell-Saunders state. Further, we consider only the $4f^5 5d$ configuration states as the high-lying states m and m' in the matrix elements (2) and (3). This is a good approximation, because the $4f^5 5d$ states are much closer in energy to the $4f^6$ states than the other electron configuration states in Sm^{2+}. Then, the line strength of the ${}^5D_0$-${}^7F_2$ transition is expressed by the sum of the terms involving the linear and the cubic components of the crystal-field potential as follows:

$$
\begin{aligned}
I(4f^6[{}^5D_0] \rightarrow 4f^6[{}^7F_2]) &= (-e)^2 \langle 4f|r|5d\rangle^2 \{\Gamma_{k=1}(4f^6[{}^5D_0] \rightarrow 4f^6[{}^7F_2]) \\
&\quad + \Gamma_{k=3}(4f^6[{}^5D_0] \rightarrow 4f^6[{}^7F_2])\}
\end{aligned}
\tag{5}
$$

with

$$
\begin{aligned}
\Gamma_{k=1}(4f^6[{}^5D_0] \rightarrow 4f^6[{}^7F_2]) &= \frac{24}{35} E_{df}^{-2} \left(\sum_q |B'_{1q}|^2 \right) (\langle 4f^6\ {}^7F_2 \| \mathbf{U}^{(2)} \| 4f^6[{}^5D_0] \rangle \\
&\quad + \langle 4f^6\ {}^7F_2 \| \mathbf{Q}^{(2)}_{k=1} \| 4f^6[{}^5D_0] \rangle)^2
\end{aligned}
\tag{6}
$$

and

$$
\begin{aligned}
\Gamma_{k=3}(4f^6[{}^5D_0] \rightarrow 4f^6[{}^7F_2]) &= \frac{64}{1715} E_{df}^{-2} \left(\sum_q |B'_{3q}|^2 \right) (\langle 4f^6\ {}^7F_2 \| \mathbf{U}^{(2)} \| 4f^6[{}^5D_0] \rangle \\
&\quad + \langle 4f^6\ {}^7F_2 \| \mathbf{Q}^{(2)}_{k=3} \| 4f^6[{}^5D_0] \rangle)^2,
\end{aligned}
\tag{7}
$$

where

$$
\begin{aligned}
\mathbf{Q}^{(2)}_{k=1} = E_{df}^{-1} \Bigg\{ & (42)^{1/2} \zeta_f \mathbf{U}^{(2)} \mathbf{W}^{(11)0} \\
& + \frac{3}{2} \left(\frac{1}{5} \right)^{1/2} \left(\zeta_f - \frac{4}{9} \zeta_d \right) \mathbf{W}^{(11)2} + \frac{1}{2} \left(\frac{3}{5} \right)^{1/2} \zeta_f \mathbf{W}^{(12)2} \\
& - \left(\frac{3}{5} \right)^{1/2} (\zeta_f - \zeta_d) \mathbf{W}^{(13)2} \Bigg\},
\end{aligned}
\tag{8}
$$

$$
\begin{aligned}
\mathbf{Q}^{(2)}_{k=3} = E_{df}^{-1} \Bigg\{ & (42)^{1/2} \zeta_f \mathbf{U}^{(2)} \mathbf{W}^{(11)0} + \frac{3}{2} \left(\frac{1}{5} \right)^{1/2} (\zeta_f - \zeta_d) \mathbf{W}^{(11)2} \\
& + \frac{1}{2} \left(\frac{3}{5} \right)^{1/2} \zeta_f \mathbf{W}^{(12)2} - \left(\frac{3}{5} \right)^{1/2} \left(\zeta_f - \frac{1}{6} \zeta_d \right) \mathbf{W}^{(13)2} \Bigg\},
\end{aligned}
\tag{9}
$$

and

TABLE I. Values of the matrix elements $\langle WUSLJ \| \mathbf{W}^{(1\lambda)t} \| W'U'S'L'J' \rangle$ of the double tensor operators used in the calculation of the ${}^5D_0$-${}^7F_2$ transition strength. Here, W and U are the irreducible representations of the seven-dimensional rotational group R_7 and its subgroup G_2, respectively.

$$\langle 4f^6(100)(10)^7F_0 \| \mathbf{W}^{(11)0} \| 4f^6(100)(10)^7F_0 \rangle = \sqrt{\frac{2}{21}}$$

$$\langle 4f^6(100)(10)^7F_0 \| \mathbf{W}^{(11)0} \| 4f^6(111)(20)^5D_0 \rangle = -\sqrt{\frac{2}{7}}$$

$$\langle 4f^6(100)(10)^7F_0 \| \mathbf{W}^{(11)0} \| 4f^6(210)(20)^5D_0 \rangle = \frac{1}{7}$$

$$\langle 4f^6(100)(10)^7F_0 \| \mathbf{W}^{(11)0} \| 4f^6(210)(21)^5D_0 \rangle = \frac{1}{7}\sqrt{\frac{11}{3}}$$

$$\langle 4f^6(100)(10)^7F_2 \| \mathbf{W}^{(11)2} \| 4f^6(100)(10)^7F_0 \rangle = -\frac{1}{2}\sqrt{\frac{5}{7}}$$

$$\langle 4f^6(100)(10)^7F_2 \| \mathbf{W}^{(11)2} \| 4f^6(111)(20)^5D_0 \rangle = -\frac{2}{5}\sqrt{\frac{15}{7}}$$

$$\langle 4f^6(100)(10)^7F_2 \| \mathbf{W}^{(11)2} \| 4f^6(210)(20)^5D_0 \rangle = \frac{1}{35}\sqrt{30}$$

$$\langle 4f^6(100)(10)^7F_2 \| \mathbf{W}^{(11)2} \| 4f^6(210)(21)^5D_0 \rangle = \frac{1}{35}\sqrt{110}$$

$$\langle 4f^6(100)(10)^7F_2 \| \mathbf{W}^{(12)2} \| 4f^6(100)(10)^7F_0 \rangle = -\frac{5}{2}\sqrt{\frac{1}{105}}$$

$$\langle 4f^6(100)(10)^7F_2 \| \mathbf{W}^{(12)2} \| 4f^6(111)(20)^5D_0 \rangle = 0$$

$$\langle 4f^6(100)(10)^7F_2 \| \mathbf{W}^{(12)2} \| 4f^6(210)(20)^5D_0 \rangle = -\frac{6}{35}\sqrt{10}$$

$$\langle 4f^6(100)(10)^7F_2 \| \mathbf{W}^{(12)2} \| 4f^6(210)(21)^5D_0 \rangle = -\frac{3}{35}\sqrt{\frac{165}{2}}$$

$$\langle 4f^6(100)(10)^7F_2 \| \mathbf{W}^{(13)2} \| 4f^6(100)(10)^7F_0 \rangle = \sqrt{\frac{5}{21}}$$

$$\langle 4f^6(100)(10)^7F_2 \| \mathbf{W}^{(13)2} \| 4f^6(111)(20)^5D_0 \rangle = -\frac{4}{105}\sqrt{35}$$

$$\langle 4f^6(100)(10)^7F_2 \| \mathbf{W}^{(13)2} \| 4f^6(210)(20)^5D_0 \rangle = -\frac{1}{15}\sqrt{10}$$

$$\langle 4f^6(100)(10)^7F_2 \| \mathbf{W}^{(13)2} \| 4f^6(210)(21)^5D_0 \rangle = 0$$

$$\langle 4f|r|5d \rangle = \int_0^\infty R(4f)rR(5d)dr. \qquad (10)$$

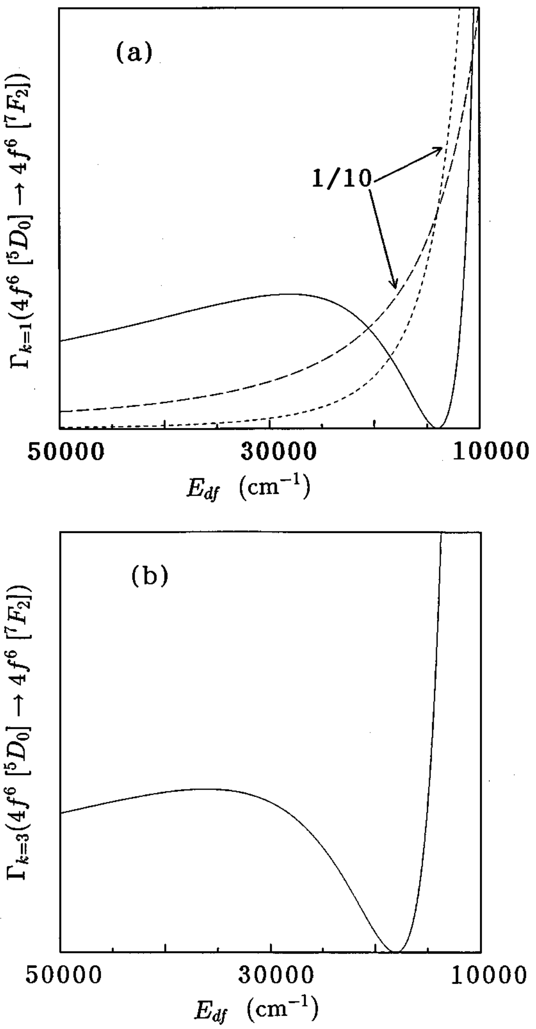

FIG. 2. (a) The values of $\Gamma_{k=1}(4f^6[{}^5D_0] \rightarrow 4f^6[{}^7F_2])$ and (b) $\Gamma_{k=3}(4f^6[{}^5D_0] \rightarrow 4f^6[{}^7F_2])$ as a function of E_{df}. The contributions of only the Judd-Ofelt mechanism and only the Wybourne-Downer mechanism are shown in (a) by the dashed and dotted lines, respectively.

Here, $-e$, E_{df}, and $R(nl)/r$ are the electron charge, the representative energy separation between the $4f^5 5d$ and $4f^6$ electron configurations, and the radial part of the appropriate single nl-electron wave function, respectively, and ζ_f and ζ_d represent the spin-orbit coupling constants for the $4f$ and $5d$ electrons, respectively. The prime of B'_{kq} denotes that the crystal-field parameter values are obtained from the radial integral for the matrix element of V_c between the $4f^6$ and $4f^5 5d$ states. The first term $\langle \ldots \| \mathbf{U}^{(2)} \| \ldots \rangle$ and the second one $\langle \ldots \| \mathbf{Q}^{(2)}_{k=j} \| \ldots \rangle$ in the second parentheses of expressions (6) and (7) result from the Judd-Ofelt and Wybourne-Downer mechanisms, respectively. Further, $\mathbf{U}^{(2)}$ is the unit tensor operator of the second rank, while $\mathbf{W}^{(1\lambda)2}$ denotes the double tensor operator of total rank 2 with rank 1 in spin space and rank λ in orbit space, and the reduced matrix element of its single-particle component $\mathbf{w}^{(1\lambda)}$ is given by

$$\langle nl \| \mathbf{w}^{(1\lambda)} \| n'l' \rangle = (5)^{1/2}(2\lambda+1)^{1/2}\delta(n,n')\delta(l,l'). \qquad (11)$$

Although Downer, Burdick, and Sardar neglected the contribution of the linear term of the crystal-field potential,[11] we consider this, because it is not considered to be negligible.

Using $\zeta_f = 1050$ cm^{-1},[16] $\zeta_d = 1000$ cm^{-1},[21] and the Slater integral $F_2 = 330$ cm^{-1},[16] which are determined from the fitting of the energy levels of

TABLE II. Values of the matrix elements $\langle WUSLJ\|\mathbf{W}^{(1\lambda)t}\|W'U'S'L'J'\rangle$ of the double tensor operators used in the calculation of the ${}^5D_0$-${}^7F_4$ transition strength.

$$\langle 4f^6(100)(10)^7F_4\|\mathbf{W}^{(13)4}\|4f^6(100)(10)^7F_0\rangle=-\frac{1}{2}\sqrt{\frac{22}{21}}$$

$$\langle 4f^6(100)(10)^7F_4\|\mathbf{W}^{(13)4}\|4f^6(111)(20)^5D_0\rangle=-\frac{1}{21}\sqrt{154}$$

$$\langle 4f^6(100)(10)^7F_4\|\mathbf{W}^{(13)4}\|4f^6(210)(20)^5D_0\rangle=-\frac{1}{6}\sqrt{11}$$

$$\langle 4f^6(100)(10)^7F_4\|\mathbf{W}^{(13)4}\|4f^6(210)(21)^5D_0\rangle=0$$

$$\langle 4f^6(100)(10)^7F_4\|\mathbf{W}^{(14)4}\|4f^6(100)(10)^7F_0\rangle=-\frac{1}{2}\sqrt{\frac{10}{7}}$$

$$\langle 4f^6(100)(10)^7F_4\|\mathbf{W}^{(14)4}\|4f^6(111)(20)^5D_0\rangle=-\frac{44}{21}\sqrt{\frac{5}{42}}$$

$$\langle 4f^6(100)(10)^7F_4\|\mathbf{W}^{(14)4}\|4f^6(210)(20)^5D_0\rangle=\frac{253}{1470}\sqrt{\frac{5}{3}}$$

$$\langle 4f^6(100)(10)^7F_4\|\mathbf{W}^{(14)4}\|4f^6(210)(21)^5D_0\rangle=\frac{44}{245}\sqrt{55}$$

$$\langle 4f^6(100)(10)^7F_4\|\mathbf{W}^{(15)4}\|4f^6(100)(10)^7F_0\rangle=\frac{1}{3}\sqrt{\frac{15}{7}}$$

$$\langle 4f^6(100)(10)^7F_4\|\mathbf{W}^{(15)4}\|4f^6(111)(20)^5D_0\rangle=-\frac{2}{15}\sqrt{\frac{5}{7}}$$

$$\langle 4f^6(100)(10)^7F_4\|\mathbf{W}^{(15)4}\|4f^6(210)(20)^5D_0\rangle=\frac{1}{105}\sqrt{10}$$

$$\langle 4f^6(100)(10)^7F_4\|\mathbf{W}^{(15)4}\|4f^6(210)(21)^5D_0)\rangle=-\frac{3}{70}\sqrt{\frac{30}{11}}$$

the Sm^{2+} ion, we obtain $\langle 4f^6\,{}^7F_2\|\mathbf{U}^{(2)}\|4f^6[{}^5D_0]\rangle=0.0636$ and $\langle 4f^6\,{}^7F_2\|\mathbf{Q}^{(2)}_{k=1}\|4f^6[{}^5D_0]\rangle=-894E_{df}^{-1}$, and $\langle 4f^6\,{}^7F_2\|\mathbf{Q}^{(2)}_{k=3}\|4f^6[{}^5D_0]\rangle=-1149E_{df}^{-1}$ (E_{df} in cm^{-1}). For the evaluations of these values, we have assumed the hydrogenic ratios for the Slater integrals $F_{2,4,6}$ and used the values of the double tensor operators shown in Table I. Further, we have taken only the dominant linkage of $\langle 4f^6\,{}^7F_2\|\mathbf{U}^{(2)}\|4f^6\,{}^7F_0\rangle\langle 4f^6\,{}^7F_0\|\mathbf{W}^{(11)0}\|4f^6[{}^5D_0]\rangle$ for the first operator in Eqs. (8) and (9). Thus, expressions (6) and (7) are written, respectively, as

$$\Gamma_{k=1}(4f^6[{}^5D_0]\rightarrow 4f^6[{}^7F_2]) =\frac{24}{35}\left(\sum_q |B'_{1q}|^2\right)E_{df}^{-2}(0.0636-894E_{df}^{-1})^2 \quad (12)$$

and

$$\Gamma_{k=3}(4f^6[{}^5D_0]\rightarrow 4f^6[{}^7F_2]) =\frac{64}{1715}\left(\sum_q |B'_{3q}|^2\right)E_{df}^{-2}(0.0636-1149E_{df}^{-1})^2. \quad (13)$$

Figures 2(a) and 2(b) show the values of $\Gamma_{k=1}(4f^6[{}^5D_0]\rightarrow 4f^6[{}^7F_2])$ and $\Gamma_{k=3}(4f^6[{}^5D_0]\rightarrow 4f^6[{}^7F_2])$ as a function of E_{df}. When we consider the contribution from either of the Judd-Ofelt mechanism or the Wybourne-Downer one, the squared transition matrix element increases monotonically with decrease of E_{df}. However, as is obvious from Figs. 2(a) and 2(b), both the ${}^5D_0$-${}^7F_2$ transition strength of Sm^{2+} arising from the linear and the cubic terms of the crystal-field potential do not. This is because of the cross terms between the matrix elements with the opposite signs to each other, i.e., $\langle\ldots\|\mathbf{U}^{(2)}\|\ldots\rangle$ and $\langle\ldots\|\mathbf{Q}^{(2)}_{k=j}\|\ldots\rangle$ ($j=1,3$), in expressions (6) and (7). Namely, the interference between the Judd-Ofelt and Wybourne-Downer mechanisms causes the cancellation of the matrix elements due to the two mechanisms. Furthermore, this cancellation in $\Gamma_{k=1}$ and $\Gamma_{k=3}$ is remarkable for E_{df} of $\sim$20 000 cm^{-1}, which roughly agrees with the representative energy separation between the $4f^55d$ and $4f^6$ configuration states estimated from the absorption spectra of the Sm^{2+}-doped materials in Refs. 1–5. Thus, the interference between the Judd-Ofelt and the Wybourne-Downer mechanisms accounts well for the fact that the ${}^5D_0$-${}^7F_2$ transition strength of the Sm^{2+} ion in solids is not enhanced even by the small energy separation between the $4f^55d$ configuration states and the $4f^6$ states concerned with the transition.

We have also calculated the strength of the ${}^5D_0$-${}^7F_4$ transition of Sm^{2+} in condensed matter. In this calculation, we used the values of the matrix elements of the double tensor operators in Tables I and II. The result shows that the cancellation of the transition matrix elements due to the two mechanisms occurs similarly to the case of the ${}^5D_0$-${}^7F_2$ transition. Indeed, the fluorescence lines of the ${}^5D_0$-${}^7F_4$ transition are rather weak in Fig. 1(a) and Refs. 4 and 14.

IV. SUMMARY

For the understanding of all the ${}^5D_0$-${}^7F_{0,2,4}$ transition strengths of Sm^{2+} in solids, we have taken into account not only the Judd-Ofelt mechanism but also the Wybourne-Downer mechanism. The energy proximity of the $4f^55d$ configuration states to the $4f^6$ states in Sm^{2+} has been found to lead to an enhancement of the transition strength for the ${}^5D_0$-${}^7F_0$ transition which is allowed by the Wybourne-Downer mechanism, but not by the Judd-Ofelt mechanism. However, it does not lead to the intensity enhancement for the ${}^5D_0$-${}^7F_{2,4}$ transitions which are allowed by both of these mechanisms. This has been attributed to the interference effect between the contributions of the Judd-Ofelt and Wybourne-Downer mechanisms to the ${}^5D_0$-${}^7F_{2,4}$ transition strengths.

ACKNOWLEDGMENTS

The authors are indebted to Dr. T. Izumitani of Hoya Corporation and Dr. S. Todoroki of NTT Corporation for providing them the HBLAN and ZBL glass samples to measure the spectra in Fig. 1, respectively.

[1] W. E. Bron and W. R. Heller, Phys. Rev. **136**, A1433 (1964).

[2] J. W. M. Verwey, G. J. Dirksen, and G. Blasse, J. Phys. Chem. Solids **53**, 367 (1992).

[3] J. W. M. Verwey and G. Blasse, J. Phys. Chem. Solids **53**, 1157 (1992).

[4] T. Izumitani and S. A. Payne, J. Lumin. **54**, 337 (1993).

[5] G. Blasse, Struct. Bonding **26**, 43 (1976).

[6] J. C. Krupa, I. Gérard, and P. Martin, J. Alloys Compounds **188**, 77 (1992).

[7] M. Tanaka and T. Kushida, Phys. Rev. B **49**, 5192 (1994).

[8] B. R. Judd, Phys. Rev. **127**, 750 (1962).

[9] G. S. Ofelt, J. Chem. Phys. **37**, 511 (1962).

[10] B. G. Wybourne, J. Chem. Phys. **48**, 2596 (1968).

[11] M. C. Downer, G. W. Burdick, and D. K. Sardar, J. Chem. Phys. **89**, 1787 (1988).

[12] G. W. Burdick, M. C. Downer, and D. K. Sardar, J. Chem. Phys. **91**, 1511 (1989).

[13] S. F. Mason, R. D. Peacock, and B. Stewart, Mol. Phys. **30**, 1829 (1975).

[14] H. V. Lauer, Jr., and F. K. Fong, J. Chem. Phys. **65**, 3108 (1976).

[15] T. Kushida, E. Takushi, and Y. Oka, J. Lumin. **12/13**, 723 (1976).

[16] G. S. Ofelt, J. Chem. Phys. **38**, 2171 (1963).

[17] For the fluorescence spectra of Eu^{3+} in solids, see for example, W. F. Krupke, Phys. Rev. **145**, 325 (1966); M. J. Weber, T. E. Varitimos, and B. H. Matsinger, Phys. Rev. B **8**, 47 (1973); S. Taboada, A. de Andrés, J. E. M. Santiuste, C. Prieto, J. L. Martinez, and A. Criado, *ibid.* **50**, 9157 (1994).

[18] For the fluorescence spectra of Sm^{2+} in solids, see, for example, Refs. 2–4, 14, and M. Nogami and Y. Abe, Appl. Phys. Lett. **64**, 1227 (1994).

[19] M. Tanaka, G. Nishimura, and T. Kushida, Phys. Rev. B **49**, 16 917 (1994).

[20] G. Blasse and A. Bril, Philips Res. Rep. **21**, 368 (1966).

[21] A. Yanase, J. Phys. Soc. Jpn. **42**, 1680 (1977).